Published OnlineFirst May 4, 2010; DOI: 10.1158/0008-5472.CAN-09-3848

Cancer Research

Three-Dimensional Cell Growth Confers Radioresistance by Chromatin Density Modification

Katja Storch[1], Iris Eke[1], Kerstin Borgmann[4], Mechthild Krause[2], Christian Richter[1], Kerstin Becker[3], Evelin Schröck[3], and Nils Cordes[1]

Abstract

Cell shape and architecture are determined by cell-extracellular matrix interactions and have profound effects on cellular behavior, chromatin condensation, and tumor cell resistance to radiotherapy and chemotherapy. To evaluate the role of chromatin condensation for radiation cell survival, tumor cells grown in three-dimensional (3D) cell cultures as xenografts and monolayer cell cultures were compared. Here, we show that increased levels of heterochromatin in 3D cell cultures characterized by histone H3 deacetylation and induced heterochromatin protein 1α expression result in increased radiation survival and reduced numbers of DNA double strand breaks (DSB) and lethal chromosome aberrations. Intriguingly, euchromatin to heterochromatin–associated DSBs were equally distributed in irradiated 3D cell cultures and xenograft tumors, whereas irradiated monolayer cultures showed a 2:1 euchromatin to heterochromatin DSB distribution. Depletion of histone deacetylase (HDAC) 1/2/4 or application of the class I/II pharmacologic HDAC inhibitor LBH589 induced moderate or strong chromatin decondensation, respectively, which was translated into cell line–dependent radiosensitization and, in case of LBH589, into an increased number of DSBs. Neither growth conditions nor HDAC modifications significantly affected the radiation-induced phosphorylation of the important DNA repair protein ataxia telangiectasia mutated. Our data show an interrelation between cell morphology and cellular radiosensitivity essentially based on chromatin organization. Understanding the molecular mechanisms by which chromatin structure influences the processing of radiation-induced DNA lesions is of high relevance for normal tissue protection and optimization of cancer therapy. *Cancer Res; 70(10); 3925–34. ©2010 AACR.*

Introduction

Cell shape and architecture have profound impact on cellular behavior (1). Models of normal and transformed cells impressively showed that three-dimensional (3D) growth in an extracellular matrix (ECM) substantially modifies gene and protein expression, survival, proliferation, differentiation, and metabolism compared with conventional monolayer cell cultures (2–4). These findings suggest that cell morphology fundamentally determines tissue homeostasis and cellular responsiveness to external stress signals in a microenvironment-specific context. A prime example of this phenomenon is enhanced tumor cell resistance to radiotherapy and chemotherapy in 3D cultured cells (5–7).

In a 3D environment, cells show a round morphology resulting from a tightly controlled interplay between cell-ECM–mediating focal adhesions and the actin cytoskeleton (8). Through physical forces between cell membrane, actin cytoskeleton, and nuclear matrix, cell morphology is considered to contribute to chromatin reorganization and gene expression. In mammary epithelial cells, 3D growth reduced histone H3 and H4 acetylation and gene expression (3, 9), indicating highly condensed chromatin, termed heterochromatin, in contrast to less compacted chromatin, termed euchromatin (10). Acetylation, methylation, and phosphorylation are specific histone protein modifications controlling the folding and condensation status of chromatin (10). Counterbalanced by histone acetyltransferases (HAT), the protein family of histone deacetylases (HDAC) is critically involved in these post-translational modifications inevitable for DNA-dependent processes such as transcription and replication (11).

In cancer, abundant HDAC activity especially represses expression of diverse tumor suppressor genes such as p53 and von Hippel-Lindau, thereby inducing tumor cell proliferation and tumor progression (12). Preclinical and clinical evaluation of the potential of HDACs as cancer targets using pharmacologic inhibitors showed cytotoxic effects in hematopoietic malignancies and cytostatic effects in cells from solid tumors (11, 13–15). Based on the function of HDACs

Authors' Affiliations: [1]OncoRay-Center for Radiation Research in Oncology, [2]Department of Radiation Oncology, and [3]Institute for Clinical Genetics, Medical Faculty Carl Gustav Carus, Dresden University of Technology, Dresden, Germany; and [4]Laboratory of Radiobiology and Experimental Radiooncology, Clinic of Radiotherapy and Radiooncology, University Medical Center Hamburg-Eppendorf, Hamburg, Germany

Note: Supplementary data for this article are available at Cancer Research Online (http://cancerres.aacrjournals.org/).

Corresponding Author: Nils Cordes, OncoRay-Center for Radiation Research in Oncology, Medical Faculty Carl Gustav Carus, Dresden University of Technology, Fetscherstrasse 74/PF 41, 01307 Dresden, Germany. Phone: 49-351-458-7401; Fax: 49-351-458-7311; E-mail: Nils.Cordes@Oncoray.de.

doi: 10.1158/0008-5472.CAN-09-3848

Published OnlineFirst May 4, 2010; DOI: 10.1158/0008-5472.CAN-09-3848

in chromatin organization and gene expression, HDAC inhibitors, such as the HDAC class I/II inhibitor LBH589 (Panobinostat), have successfully been tested as radiosensitizing agents (16–20). Mechanistically, the radiosensitizing ability of HDAC inhibitors might arise from the reduction of heterochromatin, an event proposed to crucially affect radiogenic induction and repair of DNA double strand breaks (DSB; ref. 21). Recent findings showed a mechanistic connection between the heterochromatin factors HDAC1/2, heterochromatin protein 1α (HP1α), and ataxia telangiectasia mutated (ATM)–dependent repair of radiation-induced DSBs in eukaryotic cells (22). HP1α is a nonhistone chromosomal protein participating in gene silencing at heterochromatic regions (23). Through its chromodomain, HP1α interacts with histone H3. p53 binding protein 1 (p53BP1), another nonhistone chromosomal protein involved in the DNA damage response (24), has been shown to sense DSBs in an ATM-independent manner and to interact with HDAC4 (25).

DSBs induced by ionizing radiation are life-threatening DNA lesions. Their inaccurate and inefficient repair results in chromosomal aberrations, loss of genome integrity, and cell death (26, 27). In response to DNA damage, one of the first steps is the phosphoinositide 3-kinase–related protein kinase (PIKK)–dependent phosphorylation of the conserved serine (S) 139 amino acid residue at the COOH terminus of histone H2AX, which is called γH2AX (28, 29). ATM and DNA-protein kinase, as members of the PIKK family, are essential players in the DNA repair machinery (29).

In this study, the impact of growth conditions and the distribution of radiation-induced DSBs in euchromatin and heterochromatin on radiation survival were evaluated in 3D laminin-rich ECM cell cultures, xenograft tumors, and monolayer cell cultures. Here, we show that increased radiation survival of 3D-grown cells results from a larger amount of heterochromatin, a differential dissemination of euchromatin to heterochromatin–associated DSBs in 3D versus two-dimensional (2D), and a lower number of lethal chromosome aberrations. Mechanistically, depletion of HDAC1/2/4 or application of the class I/II pharmacologic HDAC inhibitor LBH589 induced moderate or strong chromatin decondensation, respectively, which translated into enhanced cell line–dependent radiation sensitivity and, in the case of LHB589, into an increased number of DSBs.

Materials and Methods

Antibodies and reagents. Antibodies against ATM-S1981 and Tri-methyl K9 H3 (Abcam); HIF1α (BD); ATM, HP1α, histone H3, HDAC1, HDAC2, and HDAC4 (Cell Signaling); ATM (GeneTex); β-actin (Sigma); acetyl-histone H3, histone γH2AX-S139 (Upstate); p53BP1 (Acris); horseradish peroxidase–conjugated donkey anti-rabbit and sheep anti-mouse (Amersham); Alexa Fluor 594 anti-mouse, Alexa Fluor 488 anti-rabbit, and Alexa Fluor 594 phalloidin (Invitrogen); and anti-mouse pimonidazole (NPI) were purchased as indicated. Enhanced chemiluminescent reagent was from Amersham, G418 from Calbiochem, Oligofectamine from Invitrogen, dimethyl sulfoxide (DMSO) from Applichem, and deferroxamin from Sigma. Vectashield mounting medium with 4,5-diamino-2-phenylindole (DAPI) was from Alexis.

Cell culture, radiation exposure, and radiation dosimetry of 3D and 2D cell cultures. Human lung carcinoma cell line A549 was purchased from American Tissue Culture Collection. UTSCC15 human head and neck squamous cell carcinoma cells were kindly provided by R. Grenman (Turku University Central Hospital, Finland). Cells were cultured in Dulbecco's modified Eagle's medium (DMEM) containing glutamax-I supplemented with 10% fetal calf serum and 1% nonessential amino acids (PAA) at 37°C in a humidified atmosphere containing 7% CO_2. In all experiments, asynchronously growing cells were used. Irradiation was delivered at room temperature using 2 to 6 Gy single doses of 200-kV X-rays (Yxlon Y.TU 320; Yxlon; dose rate ~1.3 Gy/min at 20 mA) filtered with 0.5 mm Cu. The absorbed dose was measured using a Duplex dosimeter (PTW). Absolute dosimetry was determined for different irradiation setups under 2D and 3D cell culture conditions (see Supplementary Information).

Generation of HP1α-EGFP transfectants. HP1α PCR fragment (hHP1α-N1-fw: 5′-gg-GGTACCATGGGAAAGAAAACCAAGCGG-3′; hHP1α-N1-rev: 5′-cg-GGATCCCGGCTCTTTGCTGTTTCTTTCTCT-3′) was amplified using a cDNA construct encoding for human HP1α (a kind gift from H. Tagami, Nagoya City University, Japan; ref. 30), followed by ligation of HP1α in frame into *Kpn*I/*Bam*HI restriction sites of pEGFP-N1 expression vector (pHP1α-EGFP-N1). Stable transfection and selection was performed as described (7). This approach was used to monitor the intracellular/nuclear localization of HP1α.

Immunofluorescence staining. For detection of DSBs, the phosphorylated H2AX-S139 (γH2AX)/p53 binding protein 1 (p53BP1) focus assay was performed as published (ref. 31; see Supplementary Information). γH2AX/p53BP1–positive and γH2AX-positive nuclear foci of at least 150 cells were counted microscopically with an Axioscope 2 plus fluorescence microscope (Zeiss) and defined as DSBs.

Colony formation assay under 2D and 3D cell culture conditions. The 2D and 3D colony formation assay was applied for measurement of clonogenic cell survival as published (ref. 6; see Supplementary Information). Where indicated, cells were incubated with the HDAC inhibitor LBH589 (10–50 μmol/L) or DMSO as control for 24 hours before irradiation until 4 hours after irradiation. The inhibitor was removed by washing three to four times with PBS (2D) or DMEM (3D). Each point on the survival curves represents the mean surviving fraction from at least three independent experiments.

Chromosome aberrations. Chromosomal damage was assessed by the G0 assay as described previously (32) and by spectral karyotyping (ref. 33; see Supplementary Information).

siRNA-mediated knockdown. siRNA knockdown was performed as published (ref. 6; see Supplementary Information).

HDAC inhibition by LBH589. LBH589, kindly provided by Novartis Pharma AG, is a cinnamic hydroxamic acid analogue class I and II HDAC inhibitor (34). LBH589 was

Published OnlineFirst May 4, 2010; DOI: 10.1158/0008-5472.CAN-09-3848

dissolved in DMSO to a concentration of 1 mmol/L and stored at −20°C.

Total protein extracts and Western blotting. Cells grown either on or in laminin-rich ECM were irradiated, where indicated, with 0 to 6 Gy and/or treated with LBH589 (10–50 μmol/L) or DMSO as control. Cell lysis, SDS-PAGE, Western blotting, and protein detection were performed as published (ref. 6; see Supplementary Information).

Animals and tumor model, irradiation, and histology. The experiments were performed using 7- to 14-week-old male and female NMRI (nu/nu) mice (Experimental Centre of the Medical Faculty Carl Gustav Carus, Technische Universität Dresden) as published (ref. 35; see Supplementary Information). The animal facilities and the experiments were approved according to institutional guidelines and the German animal welfare regulations. For the experiments, small tumor pieces were transplanted s.c. into the right hind leg of anaesthetized mice. Each group (control, irradiation) of A549 xenograft tumors contained five to eight animals. Treatments started at a tumor diameter of 7 mm. The hypoxia marker pimonidazole (NPI) was injected i.p. (0.1 mg/g body weight, dissolved at 10 mg/mL in NaCl) 1 hour before 4-Gy irradiation using 200-kV X-rays (0.5 mm Cu; dose rate ~1 Gy/min) under ambient blood flow conditions (35). Animals were sacrificed by cervical dislocation, and tumors were excised 24 hours after irradiation. For γH2AX and HP1α staining, the TSA kit (Invitrogen) was used according to the manufacturer's instructions and as published (36).

Statistical analysis. Data were expressed as means ± SD of at least three independent experiments. *P* values were based on the Student's *t* test, and the significance was set at 0.05.

Results

3D growth determines cell shape, histone acetylation, and HP1α expression. To examine the effects of cell growth on chromatin condensation as indicated by histone H3 acetylation and HP1α expression, we microscopically compared 2D and 3D cell cultures and found dramatic changes in cell shape and cytoskeletal architecture (Fig. 1A). In parallel to these 3D-induced morphologic changes, 3D A549, UTSCC15, and HP1α-EGFP cell cultures exhibited diminished levels of histone H3 acetylation and induced HP1α expression, indicating a higher amount of heterochromatin (Fig. 1B and C; Supplementary Fig. S1A–C). Localization of HP1α-EGFP to heterochromatic DNA was confirmed by staining of histone H3 K9 methylation (Supplementary Fig. S1D; ref. 37).

3D growth confers radioresistance evolving from a reduced number of DNA DSBs. Based on 3D-induced chromatin condensation, we next examined the influence of this induction on clonogenic radiation survival and the number of radiogenic residual DSBs (rDSB) and of chromosomal aberrations in 3D in comparison with 2D. Both A549 and UTSCC15 cells showed significant ($P < 0.01$) higher radiation survival under 3D than under 2D conditions (Fig. 2A), which correlated with a diminished number of γH2AX/p53BP1–positive foci at 24 hours after irradiation (representing rDSBs; Fig. 2B; Supplementary Fig. S2). Unrepaired DSBs can be transferred into chromosomal aberrations. Therefore, metaphase spreads were screened for excess chromosomal fragments arising from terminal or interstitial deletions and dicentric chromosomes. Radiation dose dependently, the number of chromosomal fragments measured by the G0 assay (Fig. 2C) and spectral karyotyping analysis (Supplementary Fig. S3; Supplementary Table S1) was significantly ($P < 0.05$) lower in 3D compared with 2D cell cultures, which correlated with both radiation survival (Supplementary Fig. S4A) and number of foci (Supplementary Fig. S4B). Differences in dose distribution and oxygenation in 3D and 2D cell culture models, which are likely to influence the aforementioned end points, were excluded by radiation dosimetry (Supplementary Figs. S5–7; Supplementary Tables S2 and S3) and measurement of mRNA expression of hypoxia-related genes by DNA microarrays (Supplementary Tables S4–7; Supplementary Fig. S6) and HIF1α expression by Western blotting (Supplementary Fig. S9A). Due to transient HIF1α induction in 3D cell cultures relative to 2D, we excluded the impact of this

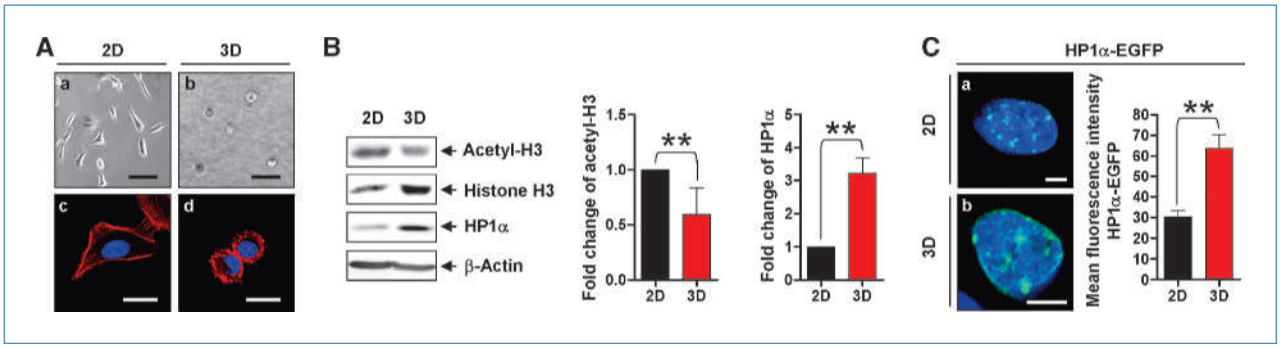

Figure 1. Growth conditions determine cell morphology and chromatin condensation. A, phase-contrast (a and b; bar, 50 μm) and immunofluorescence images (c and d; bar, 10 μm) of F-actin (red) and DAPI (blue) of 2D and 3D laminin-rich ECM A549 cell cultures. B, Western blot analysis of acetyl-H3, histone H3, and HP1α in A549 cells. Normalization to β-actin follows densitometry ($n = 3$). C, fluorescence images (a and b; bar, 5 μm) of HP1α-EGFP (green; DAPI, blue) and quantification of HP1α-EGFP fluorescence intensity in transfectants. Means ± SD ($n = 15$) and Student's *t* test comparing 3D versus 2D conditions. **, $P < 0.01$.

Published OnlineFirst May 4, 2010; DOI: 10.1158/0008-5472.CAN-09-3848

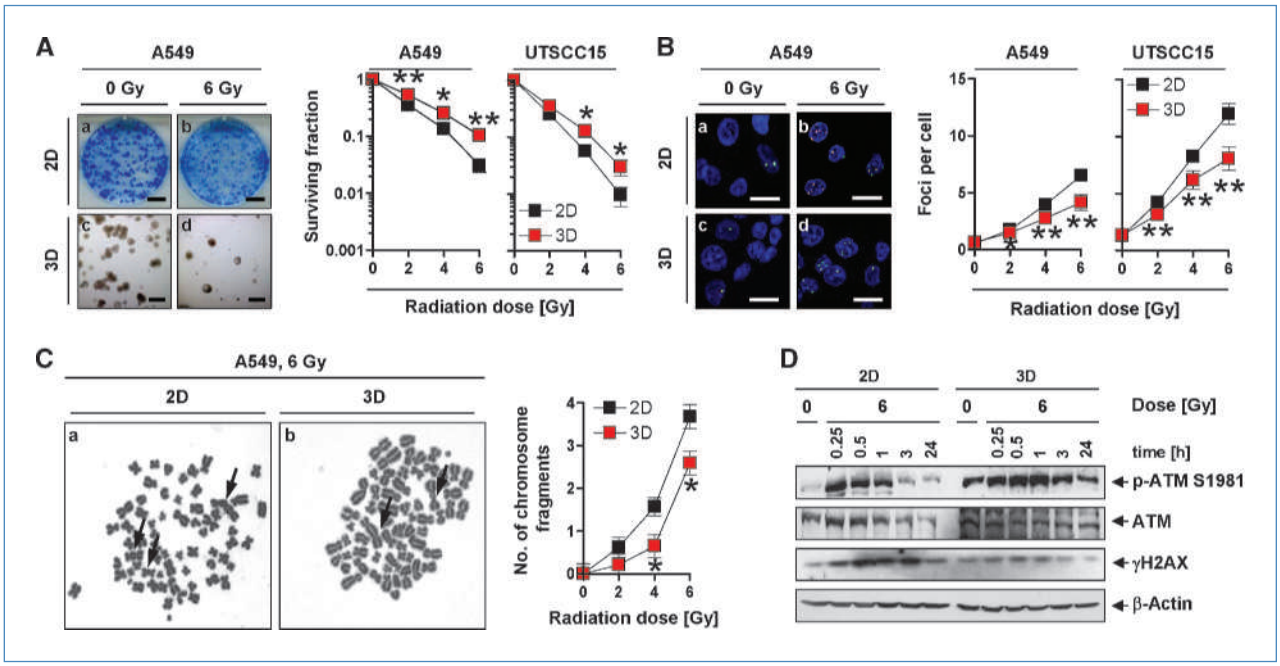

Figure 2. 3D growth conditions confer cellular resistance to ionizing radiation. A, photographs illustrate growth characteristics of cell colonies 8 days after 0 or 6 Gy (a–d; bar, 200 μm). 2D and 3D clonogenic radiation survival of A549 and UTSCC15 cells irradiated with single doses of X-rays (0–6 Gy; $n = 3$). B, photographs display γH2AX/p53BP1 double staining for rDSBs (a–d; bar, 20 μm). Number of γH2AX/p53BP1–positive foci (at least 150 nuclei; representing rDSBs at 24 hours after irradiation) is microscopically counted ($n = 3$). C, images of metaphase spread from nonirradiated or 6-Gy-irradiated 2D and 3D cell cultures, and analysis of metaphase fragments ($n = 3$). D, Western blot analysis of ATM protein expression and S1981 phosphorylation and γH2AX in 2D and 3D cultured cells at indicated time points after radiation with 6 Gy X-rays. Means ± SD and Student's t test comparing 3D versus 2D conditions. *, $P < 0.05$; **, $P < 0.01$.

induction on radiation sensitivity by performing clonogenic assays at 24 and 48 hours after plating (Supplementary Fig. S9B).

As 3D-dependent chromatin condensation might affect induction and repair of radiogenic DSBs, DSB repair kinetic was examined between 30 minutes up to 24 hours after a 1-Gy irradiation. The rate of radiation-induced foci was significantly ($P < 0.01$) lower in 3D than in 2D at 30 minutes and 2 hours postirradiation (Supplementary Fig. S10). Upon normalization to the foci number at 30 minutes postirradiation, the kinetic of foci decline was revealed to be similar in 3D and 2D cell cultures (Supplementary Table 8).

We next assessed whether 3D growth conditions and elevated amounts of heterochromatin have an impact on ATM. We found ATM S1981 phosphorylation to be slightly stronger and prolonged in 6-Gy-irradiated 3D A549 cell cultures relative to 2D (Fig. 2D). Although total ATM levels remained unchanged in 3D, 2D cells revealed a diminished ATM expression at 3 and 24 hours after irradiation, which paralleled ATM S1981 dephosphorylation. Detection of γH2AX showed a strong radiogenic, time-dependent induction in 2D, whereas this induction was moderate in 3D (Fig. 2D). From these findings, we conclude that cell growth in a 3D ECM matrix transduces prosurvival effects on clonogenic radiation survival emanating from a reduced number of rDSBs and lethal chromosomal aberrations without significant differences in DNA repair.

Colocalization of radiogenic DSBs with euchromatin or heterochromatin is determined by growth conditions. Unrepaired DSBs threaten genome integrity and cell survival upon exposure to ionizing radiation. Distinguishing between euchromatin and heterochromatin, it has been hypothesized that the repair of radiation-induced DSBs in heterochromatic regions is aggravated due to their more complex nature and due to a restricted access of DNA repair proteins (38). To gain first insight into the consequences of 3D-induced heterochromatin formation for rDSBs after ionizing radiation, we examined γH2AX colocalization with HP1α in HP1α-EGFP transfectants and in A549 xenograft tumors. γH2AX foci were defined as euchromatic foci (EC), and γH2AX foci overlapping with or in vicinity to HP1α were defined as heterochromatic foci (HC; Fig. 3A; Supplementary Fig. S11). According to these definitions, irradiated 3D-grown cells exhibited a 1 EC to 1 HC foci distribution (Fig. 3B), whereas 2D cell cultures showed a 2 EC to 1 HC foci distribution (Fig. 3B; Supplementary Table S9). The analysis of A549 xenograft tumors was performed in normoxic, pimonidazole-negative tumor areas (Fig. 3C) and by normalization to the DAPI-positive nuclear area (Supplementary Fig. S12A) in the absence of significant changes in HP1α expression (Supplementary Fig. S12B). Intriguingly, the EC to HC foci dissemination in 4-Gy-irradiated A549 xenograft tumors was comparable with 3D cell cultures (Fig. 3D; Supplementary Table S9; Supplementary Fig. S12C). These results were consistent among

Published OnlineFirst May 4, 2010; DOI: 10.1158/0008-5472.CAN-09-3848

mice. Taken together, these data show great similarity in the distribution of γH2AX foci to euchromatin and heterochromatic DNA regions in 3D cell cultures and *in vivo*. Owing to the high percentage of residual euchromatin DSBs in 2D cell cultures and the strong correlation between rDSBs and radiation survival, it is tempting to speculate that the repair of euchromatic DSBs is the critical determinant of clonogenic radiation survival.

HDAC knockdown induces chromatin decondensation and affects cellular radiosensitivity cell line dependently. To mechanistically investigate the importance of heterochromatin for radiation resistance, we next sought to evaluate the effects of single and combined HDAC1, HDAC2, or HDAC4 depletion on radiation survival, histone H3 acetylation, and HP1α expression. In contrast to single and double HDAC1, HDAC2, and HDAC4 knockdown (Supplementary Figs. S13A and B and S14A and B), the triple HDAC1/2/4 knockdown resulted in concomitant histone H3 hyperacetylation and HP1α repression in 3D and 2D relative to controls (Fig. 4A). Intriguingly, this chromatin decondensation failed to enhance A549 radiosensitivity whereas it enhanced the radiosensitivity of UTSCC15 cells (Fig. 4B). A comparison of the radiogenic ATM S1981 phosphorylation in 2D versus 3D A549 and UTSCC15 cell cultures indicated minor but not significant differences (Fig. 4C). These data reveal that HDAC1, HDAC2, and HDAC4 have a cell line–specific function in chromatin decondensation and clonogenic radiation survival.

A siRNA-mediated ATM knockdown (Supplementary Fig. S15A) performed to assess the role of ATM for chromatin condensation and radiation survival showed unchanged HP1α expression in 2D and 3D in both cell lines tested, whereas elevated histone H3 acetylation was detectable in 2D UTSCC15 cell cultures (Fig. 4D). Radiation survival of A549 and UTSCC15 cells was significantly ($P < 0.05$) reduced by ATM depletion in 2D but not in 3D (Supplementary Fig. S15B).

LBH589 modifies heterochromatin marker expression and leads to radiosensitization. In addition to a genetic HDAC inhibition, we next explored the chromatin- and radiosensitivity-modifying ability of the class I/II HDAC inhibitor LBH589. Compared with DMSO controls, LBH589 showed a strong induction of histone H3 acetylation parallel to a pronounced repression of HP1α and HP1α-EGFP in a time- and concentration-dependent manner (Fig. 5A–C). This LBH589-mediated chromatin decondensation resulted in significant ($P < 0.01$) cytotoxicity in 3D and 2D (Fig. 5D). Using 25 nmol/L LBH589 was efficient to radiosensitize 2D and more potently 3D A549 cell cultures (Fig. 6A), an effect

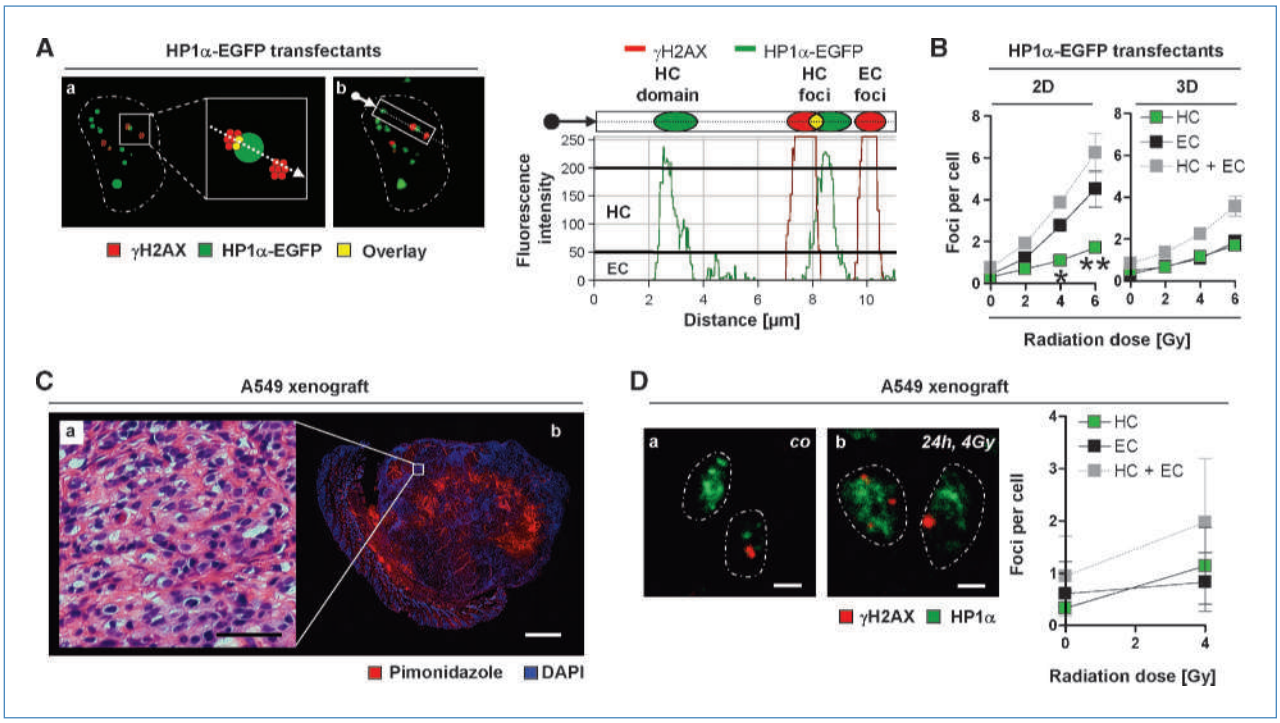

Figure 3. Heterochromatin- and euchromatin-associated rDSBs are equally distributed in 3D and *in vivo* but not in 2D. A, schematic of our definition of euchromatin- versus heterochromatin-associated γH2AX-positive foci (a; dashed line indicates nuclear area) is transferred from a representative fluorescence image (b; bar, 5 μm). The fluorescence intensity profile along the indicated arrow (in b) displays areas of heterochromatic DNA regions (HC, green), euchromatin-associated γH2AX foci (EC, red), and heterochromatin-associated γH2AX foci (yellow). B, the distribution of HC, EC, and HC+EC foci is analyzed in 3D- and 2D-grown HP1α-EGFP transfectants. Results represent means ± SD ($n = 3$). Student's *t* test compares HC versus EC foci. *, $P < 0.05$; **, $P < 0.01$. C, A549 tumor xenografts (a, H&E staining; bar, 50 μm) are stained for hypoxia using pimonidazole (b; pimonidazole, red; DAPI, blue; bar, 1 mm). D, control (a) and 4-Gy irradiated (b) tumors are examined for γH2AX foci in association with HP1α (bar, 5 μm). Distribution of HC, EC, and HC+EC foci in A549 tumor xenografts 24 hours after irradiation with 4 Gy. Results are means ± SD ($n = 5$).

Published OnlineFirst May 4, 2010; DOI: 10.1158/0008-5472.CAN-09-3848

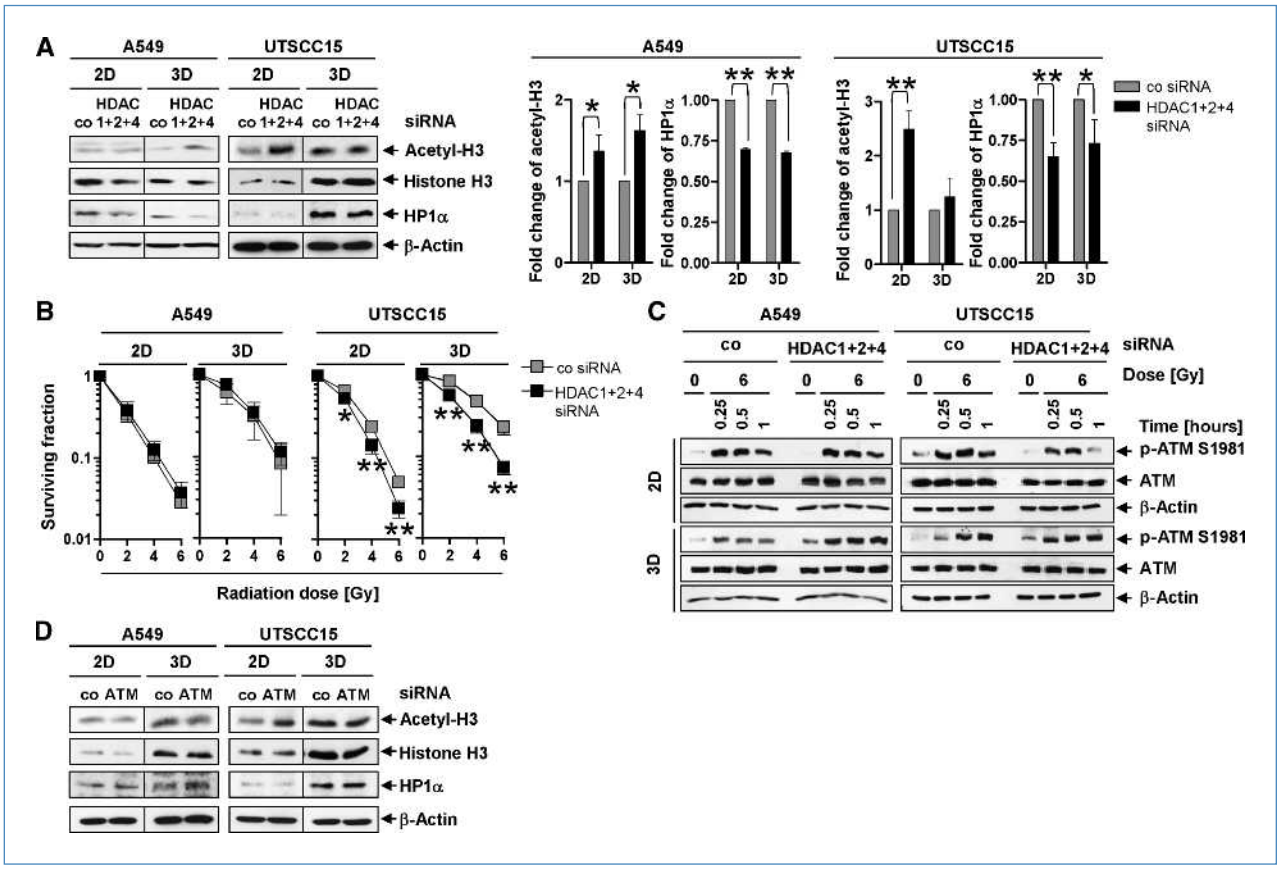

Figure 4. Combined HDAC1/2/4 depletion alters chromatin marker expression and radiosensitivity cell line dependently. A, effects of HDAC1/2/4 knockdown on histone H3 acetylation and HP1α expression analyzed by Western blotting including densitometry and normalization to β-actin. Results represent means ± SD ($n = 3$). Student's t test compares HDAC siRNA versus control siRNA. B, 2D and 3D clonogenic radiation survival (0–6 Gy) determined in HDAC1/2/4-depleted cells relative to siRNA controls. Results are means ± SD ($n = 3$). Student's t test compares HDAC1/2/4 depletion versus control siRNA. C, Western blot analysis of ATM protein expression and S1981 phosphorylation in unirradiated and 6-Gy-irradiated HDAC1/2/4 knockdown cultures. D, effects of ATM knockdown on histone H3 acetylation and HP1α expression. *, $P < 0.05$; **, $P < 0.01$.

coinciding with an elevated number of DSBs (Fig. 6B). Similar to HDAC1/2/4 depletion, HDAC inhibition by LBH589 exerted marginally prolonged ATM S1981 phosphorylation in irradiated 2D in contrast to irradiated 3D cell cultures (Fig. 6C). Our observations suggest the pharmacologic HDAC inhibitor LBH589 as a potent chromatin modifier with strong cytotoxic and radiosensitizing ability in the tested cell lines.

Discussion

Growth conditions essentially contribute to the regulation of cell fate and responsiveness to external stimuli. Whether growth conditions also affect tumor cell radioresistance and radiation-induced DSBs in a chromatin-dependent manner is currently unknown. In this study, we show that increased radiation survival in a 3D microenvironment results from an elevated amount of heterochromatin, a differential dissemination of euchromatin to heterochromatin–associated DSBs in 3D and *in vivo* versus 2D and a lower number of lethal chromosomal aberrations. Mechanistically, depletion of HDAC1/2/4 or treatment with the pharmacologic HDAC inhibitor LBH589 induced moderate or strong chromatin decondensation, respectively, an event transferred into cell line–dependent enhancement of radiosensitization and, for LBH589, into an increased number of DSBs.

The integrity, function, and homeostasis of a single cell and a tissue have been shown to be critically regulated by integrin-mediated cell adhesion to ECM. Through the ECM-integrin-cytoskeleton connection, biophysical signals are thought to govern the organization of the nuclear matrix. In cooperation with biochemical cues, these actions orchestrate cell survival, proliferation, and differentiation on the basis of chromatin remodeling and gene expression (39, 40).[5] In perfect line with this are the observed differences in chromatin condensation in 3D versus 2D cell cultures and their effects on the radiation survival response. The higher amount of heterochromatin partly protects the DNA against radiation-dependent induction of DSB. Moreover, the 3D-related chromatin modifications observable in 3D cell

[5] Zschenker and Cordes, unpublished observations.

Published OnlineFirst May 4, 2010; DOI: 10.1158/0008-5472.CAN-09-3848

cultures and in tumor xenografts shift the distribution of euchromatin to heterochromatin–associated DSBs from a 2:1 to a 1:1 ratio.

Of relevance for our work in this context is the current notion that radiogenic DSB induction and repair are hampered in heterochromatic DNA regions compared with euchromatic regions and that this affects radiation survival (22, 41, 42). Accordingly, one would expect that cells with more condensed chromatin survive worse after irradiation than cells with less condensed chromatin. Surprisingly, our data show the opposite as cells growing in a 3D ECM microenvironment have more condensed chromatin and exhibit less unrepaired DSBs in total relative to 2D. Moreover, in 3D, these unrepaired DSBs are equally divided to euchromatin and heterochromatin. In 2D, the total number of rDSBs is higher and distributed in a 2:1 ratio to euchromatin and heterochromatic DNA regions. Based on significant but minor discrepancy in the radiation-induced number of DSBs and the similarity in DSB repair kinetic under 3D versus 2D growth conditions, we conclude from these observations that the level of heterochromatin and the percentage of residual euchromatin DSBs are major determinants of radiation cell

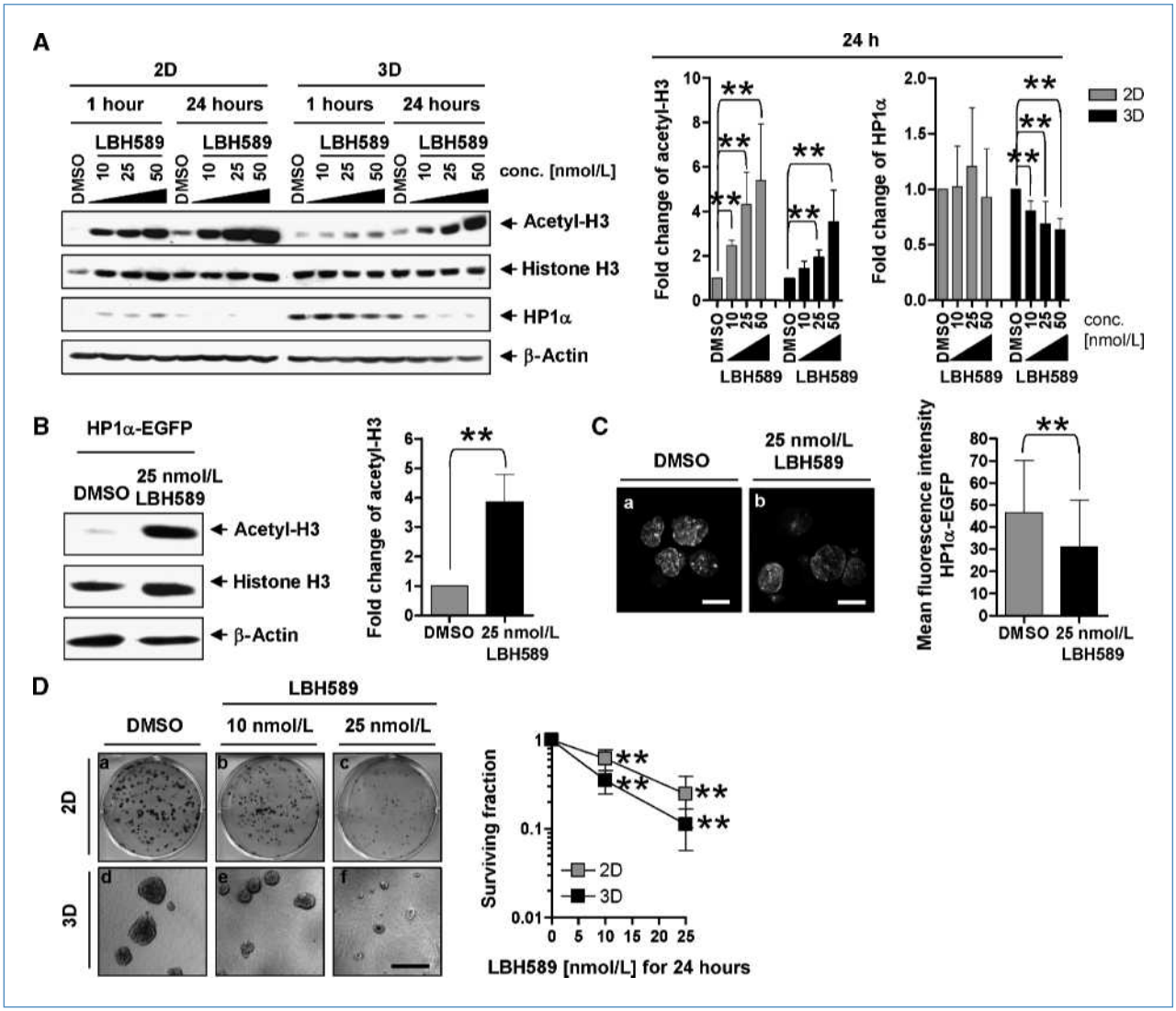

Figure 5. The HDAC inhibitor LBH589 effectively mediates chromatin decondensation and increases cell death. A, Western blot analysis of acetyl-H3, histone H3, and HP1α from LHB589-treated A549 cell lysates. Densitometric values are normalized to β-actin (n = 3). B, after a 24-hour treatment with 25 nmol/L LBH589, histone H3 acetylation is analyzed in 3D-grown HP1α-EGFP transfectants by Western blotting and densitometry. Densitometric values are normalized to β-actin (n = 3). C, immunofluorescence images and HP1α-EGFP fluorescence intensity quantification of 3D-grown HP1α-EGFP transfectants (gray, HP1α-EGFP) exposed to 25 nmol/L LBH589 for 24 hours (a and b; bar, 10 μm; DMSO as control; n = 15). D, photographs illustrate 2D (a–c; bar, 200 μm) and 3D (d–f) colony formation of LBH589-treated A549 cells 8 days after plating. Cytotoxicity data are determined in 2D and 3D cells treated with LBH589 (10 and 25 nmol/L) or DMSO. Results are expressed as means ± SD (n = 3). Student's t test compares LBH589 versus DMSO. **, $P < 0.01$.

Published OnlineFirst May 4, 2010; DOI: 10.1158/0008-5472.CAN-09-3848

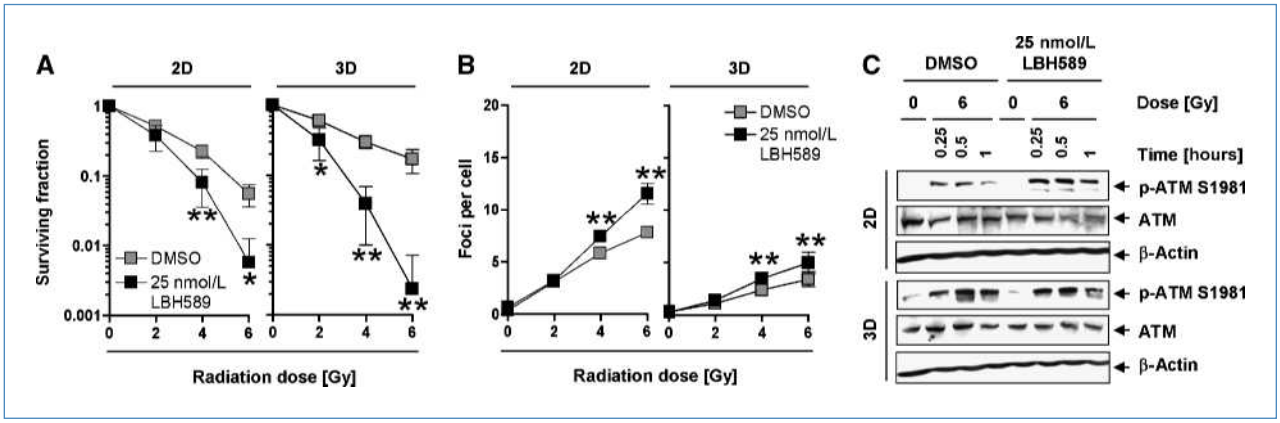

Figure 6. LBH589 sensitizes A549 cells to ionizing radiation under 2D and 3D growth conditions. A, clonogenic cell survival is analyzed in 2D- and 3D-grown cells upon combined 24-hour LBH589 treatment (DMSO as control) plus irradiation (0–6 Gy X-rays; $n = 3$). B, quantification of γH2AX/p53BP1 foci per cell is performed in LBH589/irradiation–treated cells as indicated. C, Western blot analysis of total and S1981 phosphorylated ATM upon LBH589 and 6-Gy irradiation of 2D- or 3D-grown cells. Means ± SD. Student's t test compares LBH589/irradiation versus DMSO/irradiation. *, $P < 0.05$; **, $P < 0.01$.

survival by differential regulation of DSB repair in euchromatin and heterochromatic DNA regions.

To address the mechanism through which chromatin condensation modifies radiation sensitivity and processing of radiogenic DSBs, we depleted HDAC1, HDAC2, and HDAC4 using siRNA or treated cells with the class I/II HDAC inhibitor LBH589, the spectrum of which includes HDAC1, HDAC2, and HDAC4. A triple HDAC1/2/4 knockdown was required for efficient histone H3 hyperacetylation and HP1α repression, whereas knockdown of each HDAC alone or in double combinations failed to change the histone H3 acetylation and HP1α expression pattern. HDAC1, HDAC2, and HDAC4 depletion mediated a differential, cell line–specific enhancement of cellular radiosensitivity. Without exact knowledge of the molecular mechanisms underlying this cell line–dependent differences in HDAC knockdown–mediated radiosensitization, our data support the notion of HDACs as potential cancer targets. This has already been intensively shown for several pharmacologic HDAC inhibitors *in vivo* (ref. 17, 21; reviewed in ref. 18), including the effects of LBH589 in, e.g., H460 non–small cell lung cancer (17), GIST882 gastrointestinal stromal tumor cells (43), HCT116 colon cancer cells (44), and PC3 prostate cancer cells (45). Compared with genetic HDAC1, HDAC2, and HDAC4 depletion, LBH589 treatment caused a much stronger histone H3 hyperacetylation and HP1α repression—effects less potent in 3D than in 2D. Radiation sensitivity, however, was more potently enhanced in 3D than in 2D cell cultures, which may result from a higher susceptibility of 3D cells with more condensed chromatin to the LBH589-induced chromatin decondensation. The discrepancies between siRNA-mediated HDAC1, HDAC2, and HDAC4 knockdown and LBH589 might be based on several reasons: First, decreased levels of heterochromatin and enhanced radiosensitivity coincide but are not mechanistically connected. Second, the HDAC1/2/4 knockdown–mediated chromatin decondensation encompasses particular chromatin regions not relevant for the processing of radiogenic DSBs and thus leaves clonogenic radiation survival unchanged. In contrast, LBH589 treatment circumvents this obstacle due to its broad class I/II HDAC inhibition. Third, HDACs share great functional overlap and a single, double, or triple HDAC1, HDAC2, and HDAC4 knockdown is inefficient to decondensate the chromatin to such a degree that allows radiosensitization. Whether this is due to a specific chromatin organization or an essential role of HDACs in DSB repair warrants clarification. Fourth, HDACs have both nuclear and cytoplasmic functions, as a large variety of cytoplasmic proteins are controlled by HDACs via acetylation (46, 47). It seems likely that a tightly controlled interplay between the cytoplasmic and nuclear HDAC tasks contribute to the regulation of the DNA damage response consequently determining cell fate. Fifth, different chemicals such as MS-275 or valproic acid have been shown to deactivate HDACs and were therefore termed HDAC inhibitors (18, 21, 48). As these agents are nonspecific to HDACs, the observed radiosensitization can evolve from many causes. Although the inhibitory spectrum of LBH589 comprises at least of class I (HDAC1, HDAC2, HDAC3, HDAC8) and class II (HDAC4, HDAC5, HDAC6, HDAC7, HDAC9, HDAC10) HDACs (47), the complete spectrum and its mode of action remain unresolved. Taken together, our data show that HDAC1, HDAC2, and HDAC4 are essential for chromatin remodeling and the radiation survival response in a cell line–dependent manner, and that LBH589 has a great radiosensitizing potential.

As ATM plays a critical role in DNA damage response (28), a recent study examined the specific requirement for ATM in the repair of DSBs located within or in vicinity to heterochromatin (22). Evidently, the relevance of ATM in the repair of these particular DNA lesions only became detectable when a second key molecule involved in chromatin organization such as Krüppel-associated box–associated protein 1 is deactivated (22, 49). In line with these findings, our data reveal that total ATM expression and radiation-induced S1981 phosphorylation of ATM are not significantly affected by conditions modifying chromatin condensation like 3D ECM

Published OnlineFirst May 4, 2010; DOI: 10.1158/0008-5472.CAN-09-3848

growth; siRNA-mediated HDAC1, HDAC2, and HDAC4 knockdown; or LBH589. However, requiring future examination, ATM depletion exerted radiosensitization under 2D but not 3D growth conditions. Thus, it remains to be explored how the chromatin structure exactly controls the induction, sensing, and processing of DSBs as major determinants of cell survival and which role ATM plays in this scenario upon exposure to ionizing radiation or DNA-damaging drugs.

In summary, our work shows that a 3D microenvironment exerts profound biochemical and biophysical signals resulting in increased tumor cell radioresistance. Mechanistically, an increased amount of heterochromatin, as found in 3D-grown cells, allows less DSBs and chromosomal aberrations to be induced by ionizing radiation in a HDAC1-, HDAC2-, and HDAC4-independent manner. Based on this work indicating dramatic epigenetic differences in terms of chromatin condensation between physiologic 3D and *in vivo* growth compared with artificial monolayer cultures, further in-depth analysis of the molecular mechanisms is required and may improve our understanding of normal tissue effects as well as tumor biology and tumor cell resistance to therapy.

Disclosure of Potential Conflicts of Interest

No potential conflicts of interest were disclosed.

Acknowledgments

We thank Drs. P. Jeggo and J. Dahm-Dapi for critical discussions and reading of the manuscript; Drs. T. Streichert (University Hospital Hamburg-Eppendorf, Germany) and O. Zschenker for DNA microarray analysis; A. Menegakis, K. Schumann, L. Stolz-Kieslich, A. Zielinski, and A. Frenzel for excellent technical assistance; Dr. H. Tagami (Nagoya City University, Japan) for kindly providing HP1α cDNA; Dr. R. Grenman (Turku University Central Hospital, Finland) for the UTSCC15 cell line; and Novartis (Basel, Switzerland) for the HDAC inhibitor LBH589.

Grant Support

Bundesministerium für Bildung und Forschung (BMBF-03ZIK041, N. Cordes; BMBF-03ZIK445, C. Richter).

The costs of publication of this article were defrayed in part by the payment of page charges. This article must therefore be hereby marked *advertisement* in accordance with 18 U.S.C. Section 1734 solely to indicate this fact.

Received 10/19/2009; revised 02/18/2010; accepted 03/04/2010; published OnlineFirst 05/04/2010.

References

1. Bissell MJ, Rizki A, Mian IS. Tissue architecture: the ultimate regulator of breast epithelial function. Curr Opin Cell Biol 2003;15:753–62.
2. Roskelley CD, Desprez PY, Bissell MJ. Extracellular matrix-dependent tissue-specific gene expression in mammary epithelial cells requires both physical and biochemical signal transduction. Proc Natl Acad Sci U S A 1994;91:12378–82.
3. Le Beyec J, Xu R, Lee SY, et al. Cell shape regulates global histone acetylation in human mammary epithelial cells. Exp Cell Res 2007; 313:3066–75.
4. Lelievre SA. Contributions of extracellular matrix signaling and tissue architecture to nuclear mechanisms and spatial organization of gene expression control. Biochim Biophys Acta 2009;1790:925–35.
5. Zutter MM. Integrin-mediated adhesion: tipping the balance between chemosensitivity and chemoresistance. Adv Exp Med Biol 2007;608: 87–100.
6. Eke I, Leonhardt F, Storch K, Hehlgans S, Cordes N. The small molecule inhibitor QLT0267 radiosensitizes squamous cell carcinoma cells of the head and neck. PLoS One 2009;4:e6434.
7. Hehlgans S, Eke I, Storch K, Haase M, Baretton GB, Cordes N. Caveolin-1 mediated radioresistance of 3D grown pancreatic cancer cells. Radiother Oncol 2009;92:362–70.
8. Yamada KM, Pankov R, Cukierman E. Dimensions and dynamics in integrin function. Braz J Med Biol Res 2003;36:959–66.
9. Lelievre S, Weaver VM, Bissell MJ. Extracellular matrix signaling from the cellular membrane skeleton to the nuclear skeleton: a model of gene regulation. Recent Prog Horm Res 1996;51:417–32.
10. Kouzarides T. Chromatin modifications and their function. Cell 2007; 128:693–705.
11. Xu WS, Parmigiani RB, Marks PA. Histone deacetylase inhibitors: molecular mechanisms of action. Oncogene 2007;26:5541–52.
12. Glozak MA, Seto E. Histone deacetylases and cancer. Oncogene 2007;26:5420–32.
13. Bhalla KN. Epigenetic and chromatin modifiers as targeted therapy of hematologic malignancies. J Clin Oncol 2005;23:3971–93.
14. Crisanti MC, Wallace AF, Kapoor V, et al. The HDAC inhibitor panobinostat (LBH589) inhibits mesothelioma and lung cancer cells *in vitro* and *in vivo* with particular efficacy for small cell lung cancer. Mol Cancer Ther 2009.
15. Botrugno OA, Santoro F, Minucci S. Histone deacetylase inhibitors as a new weapon in the arsenal of differentiation therapies of cancer. Cancer Lett 2009;280:134–44.
16. Zhang Y, Jung M, Dritschilo A, Jung M. Enhancement of radiation sensitivity of human squamous carcinoma cells by histone deacetylase inhibitors. Radiat Res 2004;161:667–74.
17. Geng L, Cuneo KC, Fu A, Tu T, Atadja PW, Hallahan DE. Histone deacetylase (HDAC) inhibitor LBH589 increases duration of γ-H2AX foci and confines HDAC4 to the cytoplasm in irradiated non-small cell lung cancer. Cancer Res 2006;66:11298–304.
18. Camphausen K, Tofilon PJ. Inhibition of histone deacetylation: a strategy for tumor radiosensitization. J Clin Oncol 2007;25:4051–6.
19. Ellis L, Pan Y, Smyth GK, et al. Histone deacetylase inhibitor panobinostat induces clinical responses with associated alterations in gene expression profiles in cutaneous T-cell lymphoma. Clin Cancer Res 2008;14:4500–10.
20. De Schutter H, Kimpe M, Isebaert S, Nuyts S. A systematic assessment of radiation dose enhancement by 5-aza-2′-deoxycytidine and histone deacetylase inhibitors in head-and-neck squamous cell carcinoma. Int J Radiat Oncol Biol Phys 2009;73:904–12.
21. Camphausen K, Burgan W, Cerra M, et al. Enhanced radiation-induced cell killing and prolongation of γH2AX foci expression by the histone deacetylase inhibitor MS-275. Cancer Res 2004;64:316–21.
22. Goodarzi AA, Noon AT, Deckbar D, et al. ATM signaling facilitates repair of DNA double-strand breaks associated with heterochromatin. Mol Cell 2008;31:167–77.
23. Hediger F, Gasser SM. Heterochromatin protein 1: don't judge the book by its cover! Curr Opin Genet Dev 2006;16:143–50.
24. Schultz LB, Chehab NH, Malikzay A, Halazonetis TD. p53 binding protein 1 (53BP1) is an early participant in the cellular response to DNA double-strand breaks. J Cell Biol 2000;151:1381–90.
25. Kao GD, McKenna WG, Guenther MG, Muschel RJ, Lazar MA, Yen TJ. Histone deacetylase 4 interacts with 53BP1 to mediate the DNA damage response. J Cell Biol 2003;160:1017–27.
26. Iliakis G, Wang H, Perrault AR, et al. Mechanisms of DNA double strand break repair and chromosome aberration formation. Cytogenet Genome Res 2004;104:14–20.
27. Jeggo PA, Lobrich M. DNA double-strand breaks: their cellular and clinical impact? Oncogene 2007;26:7717–9.
28. Kinner A, Wu W, Staudt C, Iliakis G. Gamma-H2AX in recognition and signaling of DNA double-strand breaks in the context of chromatin. Nucleic Acids Res 2008;36:5678–94.
29. van Attikum H, Gasser SM. Crosstalk between histone modifications during the DNA damage response. Trends Cell Biol 2009;19:207–17.

Published OnlineFirst May 4, 2010; DOI: 10.1158/0008-5472.CAN-09-3848

30. Quivy JP, Roche D, Kirschner D, Tagami H, Nakatani Y, Almouzni G. A CAF-1 dependent pool of HP1 during heterochromatin duplication. EMBO J 2004;23:3516–26.
31. Eke I, Sandfort V, Storch K, Baumann M, Roper B, Cordes N. Pharmacological inhibition of EGFR tyrosine kinase affects ILK-mediated cellular radiosensitization *in vitro*. Int J Radiat Biol 2007;83:793–802.
32. Borgmann K, Dede M, Wrona A, Brammer I, Overgaard J, Dikomey E. For X-irradiated normal human fibroblasts, only half of cell inactivation results from chromosomal damage. Int J Radiat Oncol Biol Phys 2004;58:445–52.
33. Schrock E, du Manoir S, Veldman T, et al. Multicolor spectral karyotyping of human chromosomes. Science 1996;273:494–7.
34. George P, Bali P, Annavarapu S, et al. Combination of the histone deacetylase inhibitor LBH589 and the hsp90 inhibitor 17-AAG is highly active against human CML-BC cells and AML cells with activating mutation of FLT-3. Blood 2005;105:1768–76.
35. Krause M, Prager J, Zhou X, et al. EGFR-TK inhibition before radiotherapy reduces tumour volume but does not improve local control: differential response of cancer stem cells and nontumourigenic cells? Radiother Oncol 2007;83:316–25.
36. Haase M, Gmach CC, Eke I, Hehlgans S, Baretton GB, Cordes N. Expression of integrin-linked kinase is increased in differentiated cells. J Histochem Cytochem 2008;56:819–29.
37. Maison C, Bailly D, Peters AH, et al. Higher-order structure in pericentric heterochromatin involves a distinct pattern of histone modification and an RNA component. Nat Genet 2002;30:329–34.
38. Misteli T, Soutoglou E. The emerging role of nuclear architecture in DNA repair and genome maintenance. Nat Rev Mol Cell Biol 2009;10:243–54.
39. Zoubiane GS, Valentijn A, Lowe ET, et al. A role for the cytoskeleton in prolactin-dependent mammary epithelial cell differentiation. J Cell Sci 2004;117:271–80.
40. Xu R, Nelson CM, Muschler JL, Veiseh M, Vonderhaar BK, Bissell MJ. Sustained activation of STAT5 is essential for chromatin remodeling and maintenance of mammary-specific function. J Cell Biol 2009;184:57–66.
41. Cowell IG, Sunter NJ, Singh PB, Austin CA, Durkacz BW, Tilby MJ. γH2AX foci form preferentially in euchromatin after ionising-radiation. PLoS One 2007;2:e1057.
42. Karagiannis TC, Harikrishnan KN, El-Osta A. Disparity of histone deacetylase inhibition on repair of radiation-induced DNA damage on euchromatin and constitutive heterochromatin compartments. Oncogene 2007;26:3963–71.
43. Floris G, Debiec-Rychter M, Sciot R, et al. High efficacy of panobinostat towards human gastrointestinal stromal tumors in a xenograft mouse model. Clin Cancer Res 2009;15:4066–76.
44. Fazzone W, Wilson PM, Labonte MJ, Lenz HJ, Ladner RD. Histone deacetylase inhibitors suppress thymidylate synthase gene expression and synergize with the fluoropyrimidines in colon cancer cells. Int J Cancer 2009;125:463–73.
45. Verheul HM, Salumbides B, Van Erp K, et al. Combination strategy targeting the hypoxia inducible factor-1 α with mammalian target of rapamycin and histone deacetylase inhibitors. Clin Cancer Res 2008;14:3589–97.
46. Yang XJ, Seto E. The Rpd3/Hda1 family of lysine deacetylases: from bacteria and yeast to mice and men. Nat Rev Mol Cell Biol 2008;9:206–18.
47. Witt O, Deubzer HE, Milde T, Oehme I. HDAC family: what are the cancer relevant targets? Cancer Lett 2009;277:8–21.
48. Chinnaiyan P, Cerna D, Burgan WE, et al. Postradiation sensitization of the histone deacetylase inhibitor valproic acid. Clin Cancer Res 2008;14:5410–5.
49. Goodarzi AA, Noon AT, Jeggo PA. The impact of heterochromatin on DSB repair. Biochem Soc Trans 2009;37:569–76.

Cancer Research
The Journal of Cancer Research (1916–1930) | The American Journal of Cancer (1931–1940)

AACR American Association for Cancer Research

Three-Dimensional Cell Growth Confers Radioresistance by Chromatin Density Modification

Katja Storch, Iris Eke, Kerstin Borgmann, et al.

Cancer Res 2010;70:3925-3934. Published OnlineFirst May 4, 2010.